

# Protease-Mediated Separation of Cis and Trans Diastereomers of 2(*R,S*)-benzyloxymethyl-4(*S*)-carboxylic Acid 1,3-Dioxolane Methyl Ester: Intermediates for the Synthesis of Dioxolane Nucleosides

Lana E. Janes,<sup>†</sup> Alex Cimpoaia,<sup>‡</sup> and Romas J. Kazlauskas<sup>\*,†</sup>

Department of Chemistry, McGill University, 801 Sherbrooke Street W, Montréal, Québec, Canada H3A 2K6, and BioChem Pharma, Inc., 275 Armand Frappier Boulevard, Laval, Québec, Canada H7V 4A7

Received May 6, 1999

Dioxolane nucleosides, in which an oxygen replaces the carbon in the 3' position in the ribose moiety of 2',3'-dideoxy nucleosides, are powerful antiviral and anticancer drugs. However, their synthesis remains challenging since it must control the relative and absolute stereochemistry of two stereocenters in the five-membered ring. Several promising routes yield a key intermediate dioxolane as a mixture of diastereomers (epimers at the 2-position of the dioxolane), but separation of these diastereomers by silica gel chromatography is tedious and expensive. In this paper, we report that two inexpensive, commercially available proteases— $\alpha$ -chymotrypsin and bovine pancreatic protease—discriminate between the cis and trans diastereomers of 2(*R,S*)-benzyloxymethyl-1,3-dioxolane-4(*S*)-carboxylic acid methyl ester. Although hydrolysis occurs at a carboxyl group three bonds away from the 2-stereocenter, the diastereoselectivity is high ( $D = 29\text{--}35$ , favoring trans). We discovered these selective hydrolases by screening a library of 91 commercial hydrolases with our previously developed stereoselectivity screens that use pH indicators. A small-scale  $\alpha$ -chymotrypsin-catalyzed hydrolysis of a 2:1 mixture of *cis*- and *trans*-dioxolane methyl esters yielded the desired *cis*-dioxolane methyl ester in >98% diastereomeric excess and 55% overall yield (67% was the maximum possible yield). Computer modeling of transition-state analogues of both diastereomers in the active site of  $\alpha$ -chymotrypsin suggests that stereoselectivity arises because the slow-reacting diastereomer binds in a nonproductive orientation.

## Introduction

3'-Thia- and oxa-substituted 2',3'-dideoxynucleoside analogues are an important class of antiviral and anticancer drugs. For example, the 3'-thiadideoxynucleoside, 3TC ( $\beta$ -L-(-)-2'-deoxy-3'-thiacytidine),<sup>1</sup> and the 3'-oxa-dideoxynucleosides (dioxolane nucleosides) ( $\pm$ )-dioxolane-T<sup>2</sup> inhibit human immunodeficiency virus (HIV) and hepatitis B virus (HBV), Figure 1. Similarly, the dioxolane nucleosides  $\beta$ -L- and  $\alpha$ -L-dioxolane 5-(2-bromovinyl)uracil ( $\alpha/\beta$ -L-dioxolane-BVU) inhibit herpes simplex virus (HSV) type 1 and 2,<sup>3</sup> while  $\beta$ -L-(2*S*,4*S*)-dioxolane cytidine (BCH-4556), the 3'-oxa derivative of 3TC, shows anticancer activity in preclinical trials.<sup>4</sup>

Since stereoisomers of dioxolane nucleosides usually have different biological activities and toxicities, many

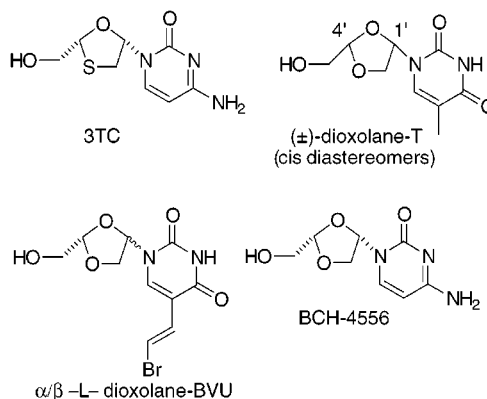


**Figure 1.** Examples of 2',3'-dideoxynucleoside analogues in clinical use or under clinical evaluation. 3TC, used in combination therapy with other drugs, is approved for the treatment of HIV and is under clinical evaluation for the treatment of HBV. ( $\pm$ )-Dioxolane-T possesses anti-HIV and anti-HBV activity, while  $\alpha/\beta$ -L-dioxolane-BVU is active against HSV-1 and HSV-2. BCH-4556 is a potent antineoplastic agent that is under clinical evaluation for the treatment of prostate, renal, and other cancers.

researchers have explored synthetic routes to pure stereoisomers of dioxolane nucleosides. These routes must control the relative and absolute stereochemistries at two potentially epimerizable centers of the dioxolane ring.

<sup>†</sup> McGill University.

<sup>‡</sup> BioChem Pharma, Inc.

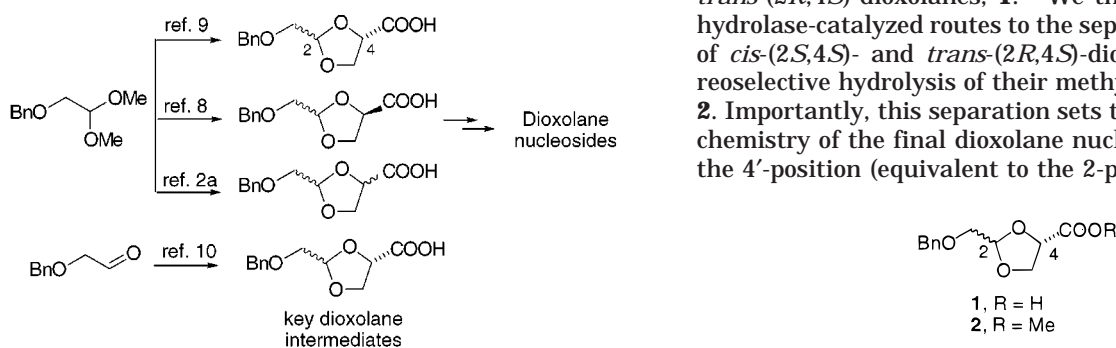
(1) Mansour, T. S.; Belleau, B.; Bednarski, K.; Breining, T.; Brown, W. L.; Cimpoaia, A.; DiMarco, M.; Dixit, D. M.; Evans, C. A.; Jin, H.; Kraus, J. L.; Lafleur, D.; Lee, N.; Nguyen-Ba, N.; Siddiqui, M. A.; Tse, H. L. A.; Zacharie, B. In *Recent Advances in the Chemistry of Anti-Infective Agents*; Bentley, P. H., Ponsford, R., Eds.; Royal Society of Chemistry: Cambridge, 1993; pp 337–347. Coates, J. A. V.; Cammack, N.; Jenkinson, H. J.; Jowett, A. J.; Jowett, M. I.; Pearson, B. A.; Penn, C. R.; Rouse, P. L.; Viner, K. C.; Cameron, J. M. *Antimicrob. Agents Chemother.* **1992**, *36*, 733–739.

(2) (a) Norbeck, D. W.; Spanton, S.; Broder, S.; Mitsuya, H. *Tetrahedron Lett.* **1989**, *30*, 6263–6266. (b) Chu, C. K.; Ahn, S. K.; Kim, H. O.; Beach, J. W.; Alves, A. J.; Jeong, L. S.; Islam, Q.; Van Roey, P.; Schinazi, R. F. *Tetrahedron Lett.* **1991**, *32*, 3791–3794. (c) Kim, H. O.; Shanmuganathan, K.; Alves, A. J.; Jeong, L. S.; Beach, J. W.; Schinazi, R. F.; Chang, C.-N.; Cheng, Y.-C.; Chu, C. K. *Tetrahedron Lett.* **1992**, *33*, 6899–6902.

(3) Bednarski, K.; Dixit, D. M.; Wang, W.; Evans, C. A.; Jin, H.; Yuen, L.; Mansour, T. S. *Bioorg. Med. Chem. Lett.* **1994**, *4*, 2667–2672.

(4) Kadhim, S. A.; Bowlin, T. L.; Waud, W. R.; Angers, E. G.; Bibeau, L.; DeMuys, J.-M.; Bednarski, K.; Cimpoaia, A.; Attardo, G. *Cancer Res.* **1997**, *57*, 4803–4810. Grove, K. L.; Guo, X.; Liu, S.-H.; Gao, Z.; Chu, C. K.; Cheng, Y.-C. *Cancer Res.* **1995**, *55*, 3008–3011.

**Scheme 1. Synthetic Routes to Diastereomerically pure Dioxolane Nucleosides via Mixtures of the Key Intermediate Dioxolane Acids<sup>a</sup>**



<sup>a</sup> Each synthesis yields a mixture of diastereomers of **1** and thus requires a separation to set the configuration in the final dioxolane nucleoside.

Two routes use expensive carbohydrates as starting materials. 1,6-Anhydro- $\beta$ -L-gulose is used for the synthesis of L-(2*S*)-dioxolane nucleosides<sup>5</sup> and 1,6-anhydro-D-mannose is used for the synthesis of D-(2*R*)-dioxolane nucleosides.<sup>2b,6</sup> Glycolic acid and *tert*-butyldiphenylsilyl-protected glycolaldehyde is used to synthesize  $\beta$ -(2*S*)-dioxolane thymidine.<sup>7</sup> Although these procedures yield pure stereoisomers of dioxolane nucleosides, they are too lengthy and expensive for large-scale synthesis.

Routes starting from less expensive carbohydrates set only one stereocenter yielding mixtures of diastereomers of a key intermediate, 2-benzyloxymethyl-4-carboxylic acid 1,3-dioxolanes. Combining benzyloxyacetaldehyde dimethyl acetal with D-mannitol,<sup>8</sup> L-ascorbic acid,<sup>9</sup> or ( $\pm$ )-methyl glycerate<sup>2a</sup> or combining benzyloxyacetaldehyde with 2,3-*O*-isopropylidene-(*S*)-glyceric acid methyl ester<sup>10</sup> yield, after a few steps, the diastereomers in Scheme 1. Separation of the mixtures of diastereomers by silica gel chromatography or fractional crystallization sets the stereochemistry at the 2-position. Next, oxidative decarboxylation to their 4-acetates prepares the dioxolanes for coupling to a base with a Lewis acid catalyst, but destroys the stereochemistry at the 4-position.<sup>11</sup> A second separation of diastereomers resets the stereochemistry at the 4-position (equivalent to the 1'-position in the final dioxolane nucleoside).

Among the different 2-benzyloxymethyl-1,3-dioxolane-4-carboxylic acids in Scheme 1, we focused on the *cis*-(2*S*,4*S*)-dioxolane, a key intermediate in the synthesis of BCH-4556. Starting from benzyloxyacetaldehyde and

2,3-*O*-isopropylidene-(*S*)-glyceric acid methyl ester yields, after several steps and saponification of the methyl esters, an approximately 2:1 mixture of *cis*-(2*S*,4*S*)- and *trans*-(2*R*,4*S*)-dioxolanes, **1**.<sup>2a</sup> We therefore focus upon hydrolase-catalyzed routes to the separation of mixtures of *cis*-(2*S*,4*S*)- and *trans*-(2*R*,4*S*)-dioxolanes by diastereoselective hydrolysis of their methyl ester precursors, **2**. Importantly, this separation sets the ultimate stereochemistry of the final dioxolane nucleoside analogue at the 4'-position (equivalent to the 2-position in **2**).

To simplify separation of these diastereomers, we explored hydrolase-catalyzed routes. Hydrolytic enzymes (hydrolases) are useful chiral catalysts for the production of enantiomerically pure alcohols and carboxylic acids. Their commercial availability, relatively low cost, and tolerance for a wide class of substrates make them attractive biocatalysts.<sup>12</sup>

Researchers have previously used enzymes to resolve enantiomers of both natural nucleosides and nucleoside analogues,<sup>13</sup> including oxathiolane and dioxolane nucleosides. Hoong et al. used pig liver esterase (PLE) to enantioselectively hydrolyze butyryl esters of ( $\pm$ )-FTC (2',3'-dideoxy-5-fluoro-3'-thiacytidine) and ( $\pm$ )-BCH-189, the racemic form of 3TC.<sup>14</sup> Storer and co-workers used a 5'-ribonucleotide phosphohydrolase from *Crotalus atrox* venom to selectively hydrolyze the (+)-monophosphate enantiomer of ( $\pm$ )-BCH-189 in >99% enantiomeric excess.<sup>15</sup> Siddiqui and co-workers used adenosine deaminase to enantioselectively deaminate purine dioxolane nucleosides in high enantiomeric excess.<sup>16</sup>

Researchers have also used enzymes to resolve key intermediates for synthesis of nucleoside analogues. Researchers from the University of Leeds and Glaxo-Wellcome used lipase from *Pseudomonas fluorescens* to prepare homochiral (ee > 90%)  $\alpha$ -acetoxy sulfides and  $\alpha,\beta$ -diacetoxy sulfides via kinetic<sup>17,18</sup> and dynamic<sup>19</sup> resolutions. Acid-catalyzed cyclization of these intermediates yields oxathiolanes, key intermediates for 3TC. Several

(12) Kazlauskas, R. J.; Bornscheuer, U. T. In *Biotechnology*; Kelly, D. R., Ed.; Wiley-VCH: Weinheim, 1998; Vol. 8a, pp 37–191. Bornscheuer, U. T.; Kazlauskas, R. J. *Hydrolases in Organic Syntheses: Regio- and Stereoselective Biotransformations*; Wiley-VCH: Weinheim, 1999. Wong, C.-H.; Whitesides, G. M. *Enzymes in Synthetic Organic Chemistry*; Pergamon: Oxford, 1994. Faber, K. *Biotransformations in Organic Chemistry*, 3rd ed.; Springer: Berlin, 1997.

(13) Hanrahan, J. R.; Hutchinson, D. W. *J. Biotechnol.* **1992**, *23*, 193–210. Prasad, A. K.; Wengel, J. *Nucleosides Nucleotides* **1996**, *15*, 1347–1359. Utagawa, T. *J. Mol. Catal. B: Enzymol.* **1999**, *6*, 215–222.

(14) Hoong, L. K.; Strange, L. E.; Liotta, D. C.; Koszalka, G. W.; Burns, C. L.; Schinazi, R. F. *J. Org. Chem.* **1992**, *57*, 5563–5565.

(15) Storer, R.; Clemens, I. R.; Lamont, B.; Noble, S. A.; Williamson, C.; Belleau, B. *Nucleosides Nucleotides* **1993**, *12*, 225–236.

(16) Siddiqui, M. A.; Brown, W. L.; Nguyen-Ba, N.; Dixit, D. M.; Mansour, T. M.; Hooker, E.; Viner, K. C.; Cameron, J. M. *Bioorg. Med. Chem. Lett.* **1993**, *3*, 1543–1546.

(17) There was complete regioselectivity for hydrolysis of the acetate group over the ester functionality with  $\alpha$ -acetoxy sulfides: Milton, J.; Brand, S.; Jones, M. F.; Rayner, C. M. *Tetrahedron: Asymmetry* **1995**, *6*, 1903–1906.

(18) Hydrolysis was completely regioselective for the primary acetate over the secondary acetate with  $\alpha,\beta$ -diacetoxy sulfides: Brand, S.; Jones, M. F.; Rayner, C. M. *Tetrahedron Lett.* **1997**, *28*, 3595–3598.

(19) Brand, S.; Jones, M. F.; Rayner, C. M. *Tetrahedron Lett.* **1995**, *36*, 8493–8496.

(5) Kim, H. O.; Schinazi, R. F.; Shanmuganathan, K.; Jeong, L. S.; Beach, J. W.; Nampalli, S.; Cannon, D. L.; Chu, C. K. *J. Med. Chem.* **1993**, *36*, 519–528.

(6) Kim, H. O.; Ahn, S. K.; Alves, A. J.; Beach, J. W.; Jeong, L. S.; Choi, B. G.; Van Roey, P.; Schinazi, R. F.; Chu, C. K. *J. Med. Chem.* **1992**, *35*, 1987–1995.

(7) Choi, W.-B.; Wilson, L. J.; Yeola, S.; Liotta, D. C. *J. Am. Chem. Soc.* **1991**, *113*, 9377–9379.

(8) Evans, C. A.; Dixit, D. M.; Siddiqui, M. A.; Jin, H.; Tse, A. H. L.; Cimpola, A.; Bednarski, K.; Breining, T.; Mansour, T. S. *Tetrahedron: Asymmetry* **1993**, *4*, 2319–2322.

(9) Belleau, B. R.; Evan, C. A.; Tse, H. L. A.; Jin, H.; Dixit, D. M.; Mansour, T. S. *Tetrahedron Lett.* **1992**, *33*, 6949–6952.

(10) Preparation of 2,3-*O*-isopropylidene-(*S*)-glyceric acid: Emons, C. H. H.; Kuster, B. F. M.; Vekeman, J. A. J. M.; Sheldon, R. A. *Tetrahedron: Asymmetry* **1991**, *2*, 359–362.

(11) Jin, H.; Tse, H. L. A.; Evans, C. A.; Mansour, T. S.; Beels, C. M.; Ravenscroft, P.; Humber, D. C.; Jones, M. F.; Payne, J. J.; Ramsay, M. V. J. *Tetrahedron: Asymmetry* **1993**, *4*, 211–214.

groups have used hydrolases in the preparation of carbocyclic nucleoside intermediates, where the ribose oxygen has been replaced with a methylene group.<sup>20</sup>

In this paper, we wanted to separate diastereomers of a key intermediate in the synthetic pathway of dioxolane nucleosides rather than the final product. The cost of each intermediate increases with each step in a synthesis so separating mixtures of the final compound is less efficient than separating intermediates of a synthetic route.

To identify selective hydrolases, traditionally a researcher carries out several small-scale kinetic resolutions with commercially available hydrolases and measures the optical purities of the reaction products. An equation developed by Sih's group permits calculations of the selectivity from the optical purities.<sup>21</sup> This method is time-consuming because it requires workup of the reactions and finding suitable analytical conditions to measure optical purities. In general, a researcher does not test all available hydrolases so potentially selective hydrolases are likely missed. To increase our chance of finding a highly selective commercial hydrolase, we used our previously developed methods to rapidly screen a library of commercial hydrolases for activity and diastereoselectivity toward the pure diastereomers of **2** using a pH indicator in 96-well plates.<sup>22</sup> Our screening has identified two hydrolases,  $\alpha$ -chymotrypsin and bovine pancreatic protease, that catalyze hydrolysis of the methyl ester but are sensitive to the configuration of the 2-stereocenter, which lies three bonds away. Hydrolysis favors the *trans* diastereomer with good diastereoselectivity ( $D = 29$ – $35$ ). We optimized these reactions and then carried out a small-scale separation of the diastereomers yielding the desired *cis*-(*2S,4S*) dioxolane, **2**, in high diastereomeric excess (>98%). This work represents our first application of our new screening method to screening for diastereoselectivity.

## Results

**Estimated Diastereoselectivity.** We first estimated the diastereoselectivity of 91 commercial hydrolases toward the *cis*-(*2S,4S*)- and *trans*-(*2R,4S*)-dioxolanes, **2**, by measuring the initial rates of hydrolysis of the two pure diastereomers separately. The ratio of the two rates is the estimated diastereoselectivity, Table 1. Note that this ratio is NOT the true diastereoselectivity, or diastereomeric ratio,  $D$ , because we measured the rates of the pure diastereomers separately.<sup>23</sup> To rapidly and

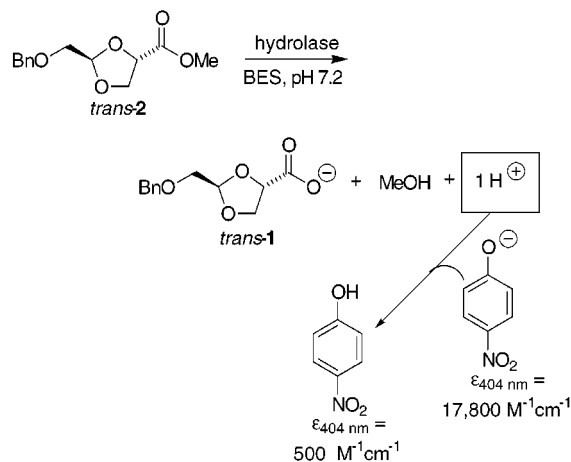


**Figure 2.** First step in the screen for estimated diastereoselectivity. Enzyme-catalyzed hydrolysis of *trans*-**2** releases a proton. We measure this rate of release with a pH indicator, 4-nitrophenol. The rate of color change of the pH indicator is proportional to the enzyme-catalyzed rate of hydrolysis using eq 1 (see Experimental Section). The second step of the screen is the same but uses *cis*-**2**. The ratio of rates of hydrolysis estimates the diastereoselectivity.

accurately determine the rates of ester hydrolysis, we used a microplate reader and pH indicator (4-nitrophenol) as described previously, Figure 2.<sup>22</sup>

Fourteen of the 91 hydrolases did not catalyze hydrolysis of either diastereomer (activity <0.01  $\mu\text{mol}/\text{min}/\text{mg}$  protein). Of the remaining 77 active hydrolases, seven showed estimated diastereoselectivities >8, all favoring the *trans*-dioxolane. Three of these hydrolases—bovine pancreas protease,  $\alpha$ -chymotrypsin, and subtilisin from *Bacillus licheniformis*—showed no detectable hydrolysis toward the *cis*-dioxolane during 20 min of screening. For these hydrolases, we report an estimated diastereoselectivity of >100. Bovine cholesterol esterase showed an estimated diastereoselectivity of 157. Protease from *Streptomyces caespitosus*, Diversa clonezyme ESL-001-02, and horse liver esterase showed modest estimated diastereoselectivities of 18, 13, and 8, respectively. Although 21 hydrolases favored the *cis*-dioxolane, their estimated diastereoselectivities were low,  $D < 1.1$ – $6.9$ . All subsequent experiments focus on six of the *trans* selective hydrolases. We omitted the Diversa clonezyme because it was expensive and showed only a moderate estimated diastereoselectivity.

**True Diastereoselectivity via Quick  $D$ .** To measure the diastereoselectivity of these six hydrolases more accurately, we extended our previously published method called “quick  $E$ ” to measure diastereoselectivity.<sup>24</sup> We refer to this screen as “quick  $D$ ”. Quick  $D$  is a spectrophotometric assay that rapidly determines the diastereoselectivity of hydrolases without measuring optical purities. We add an achiral reference compound, resorufin acetate, **3**, to the assay solutions of the pure diastereomers of **2**. This addition introduces competition between two substrates for the active site of the hydrolase in each step of the assay, thereby accounting for differences in  $K_M$  between the two diastereomers.

In the first step of the quick  $D$  screen, we measured the rates of hydrolysis of *trans*-**2** and -**3** simultaneously,

(20) Evans, C. T.; Roberts, S. M.; Shoberu, K. A.; Sutherland, A. G. *J. Chem. Soc., Perkin Trans. 1* **1992**, 589–592. Borthwick, A. D.; Biggadike, K. *Tetrahedron* **1992**, *48*, 571–623. Ohsawa, K.; Shiozawa, T.; Achiwa, K.; Terao, Y. *Chem. Pharm. Bull.* **1993**, *41*, 1906–1909. Taylor, S. J. C.; McCague, R.; Wisdom, R.; Lee, C.; Dickson, K.; Ruecroft, G.; O'Brien, F.; Littlechild, J.; Bevan, J.; Roberts, S. M.; Evans, C. T. *Tetrahedron: Asymmetry* **1993**, *4*, 1117–1128. Csuk, R.; Dörr, P. *Tetrahedron: Asymmetry* **1994**, *5*, 269–276. Mulvihill, M. J.; Gage, J. L.; Miller, M. J. *J. Org. Chem.* **1998**, *63*, 3357–3363.

(21) Chen, C.-S.; Fujimoto, Y.; Girdaukas, G.; Sih, C. J. *J. Am. Chem. Soc.* **1982**, *104*, 7294–7299.

(22) Janes, L. E.; Löwendahl, A. C.; Kazlauskas, R. J. *Chem. Eur. J.* **1998**, *4*, 2324–2330.

(23) The diastereoselectivity is the ratio of the specificity constants ( $k_{\text{cat}}/K_M$ ) for each diastereomer. By measuring initial rates of the diastereomers separately, we eliminate competitive binding between the two diastereomers. At saturating substrate concentrations, where  $[S] > K_M$ , the relative initial rates equal the relative  $K_{\text{cat}}$  values; at partially saturating conditions, where  $[S] < K_M$ , the initial rates also depend on the  $K_M$  values. Thus, the ratio of separately measured initial rates ignores some or all of the effect of  $K_M$  on diastereoselectivity. Despite this inaccuracy, the relative initial rates can provide a rapid estimate of diastereoselectivity (for example, see ref 22).

(24) Janes, L. E.; Kazlauskas, R. J. *J. Org. Chem.* **1997**, *62*, 4560–4561. Janes, L. E.; Löwendahl, A. C.; Kazlauskas, R. J. Manuscript in preparation.



**Table 1. Activity and Estimated Diastereoselectivity of Commercial Hydrolases toward *cis*-(2*S*,4*S*)- and *trans*-(2*R*,4*S*)-Dioxolane Methyl Esters, 2**

source of active hydrolase <sup>a</sup>	wt <sup>b</sup>	prot <sup>c</sup>	supplier	activity		estimated <i>D</i> <sup>e</sup>
				trans <sup>d</sup>	cis <sup>d</sup>	
<b>lipases</b>						
<i>Aspergillus niger</i>	30	0.61	<i>f</i>	0.188	0.0615	3.06 (trans)
<i>Aspergillus oryzae</i>	7.1	4.5	<i>g</i>	0.141	0.0613	2.30 (trans)
<i>Candida antarctica</i> lipase A	34	4.9	<i>h</i>	0.0457	0.0730	1.60 (cis)
<i>Candida lipolytica</i>	35	0.23	<i>f</i>	0.358	0.256	1.40 (trans)
<i>Candida rugosa</i>	31	0.35	<i>i</i>	0.358	0.225	1.59 (trans)
<i>Candida rugosa</i> (cylindracea)	37	0.71	<i>j</i>	0.777	0.327	2.38 (trans)
<i>Candida utilis</i>	4.7	0.053	<i>g</i>	5.94	1.69	3.51 (trans)
<i>Humicola</i> sp.	13	4.0	<i>h</i>	0.259	0.342	1.32 (cis)
<i>Mucor javanicus</i>	32	1.1	<i>f</i>	0.755	0.374	2.02 (trans)
<i>Mucor miehei</i>	60	1.3	<i>f</i>	0.536	0.729	1.36 (cis)
<i>Penicillin camembertii</i>	86	0.92	<i>f</i>	1.83	2.09	1.14 (cis)
<i>Penicillin roquefortii</i>	57	0.74	<i>f</i>	0.839	0.625	1.34 (trans)
<i>Pseudomonas cepacia</i>	31	3.1	<i>f</i>	0.00644	0.0199	3.09 (cis)
<i>Pseudomonas</i> sp., lipoprotein lipase	1.0	0.91	<i>g</i>	0.229	0.106	2.16 (trans)
<i>Pseudomonas</i> sp. type B, lipoprotein lipase	5.2	3.0	<i>g</i>	1.15	0.283	4.06 (trans)
<i>Rhizopus arrhizus</i>	2.1	1.7	<i>g</i>	0.168	0.176	1.05 (cis)
<i>Rhizopus javanicus</i>	44	2.7	<i>f</i>	0.142	0.0625	2.27 (trans)
<i>Rhizopus niveus</i>	57	1.9	<i>h</i>	0.408	0.503	1.23 (cis)
<i>Rhizopus oryzae</i>	53	4.1	<i>f</i>	0.0690	0.0424	1.63 (trans)
<i>Rhizopus stolonifer</i>	31	1.2	<i>f</i>	0.760	0.682	1.11 (trans)
<i>Thermus aquaticus</i>	1.1	0.29	<i>g</i>	0.238	0.154	1.55 (trans)
<b>esterases</b>						
acetylcholine esterase	0.26	0.18	<i>i</i>	0.967	0.951	1.02 (trans)
<i>Bacillus</i> sp.	1.1	0.58	<i>g</i>	0.141	0.125	1.13 (trans)
<i>Bacillus stearothermophilus</i>	1.1	0.57	<i>g</i>	1.30	1.33	1.02 (cis)
<i>Bacillus thermoglycosidarius</i>	0.82	0.76	<i>g</i>	0.671	0.334	2.01 (trans)
<b>bovine cholesterol esterase</b>	<b>9.8</b>	<b>0.99</b>	<b>k</b>	<b>2.77</b>	<b>0.0176</b>	<b>157 (trans)</b>
<i>Candida lipolytica</i>	3.5	1.4	<i>g</i>	0.183	0.229	1.25 (cis)
<i>Candida rugosa</i>	na	1.3	<i>l</i>	0.440	0.393	1.12 (trans)
cutinase from <i>Fusarium solani pisi</i> , purified	2.1	1.1	<i>m</i>	3.47	1.81	1.92 (trans)
cutinase from <i>Fusarium solani pisi</i> , crude	18	2.3	<i>m</i>	1.55	0.759	2.04 (trans)
E001	0.40	0.14	<i>n</i>	17.1	14.6	1.17 (trans)
E002	0.38	0.16	<i>n</i>	16.3	16.6	1.02 (cis)
E003	1.0	0.23	<i>n</i>	9.52	5.95	1.60 (trans)
E004	1.0	0.29	<i>n</i>	6.20	7.15	1.15 (cis)
E005	1.0	0.27	<i>n</i>	11.9	6.61	1.80 (trans)
E006	0.64	0.13	<i>n</i>	13.2	5.37	2.46 (trans)
E007	2.1	0.97	<i>n</i>	1.77	1.49	1.19 (trans)
E008	1.0	0.18	<i>n</i>	15.8	9.59	1.65 (trans)
E009	1.0	0.37	<i>n</i>	2.36	1.70	1.39 (trans)
E010	1.0	0.26	<i>n</i>	8.54	11.4	1.33 (cis)
E011	0.80	0.22	<i>n</i>	10.3	5.62	1.83 (trans)
E013	1.0	0.24	<i>n</i>	4.74	3.12	1.52 (trans)
E014	1.0	0.31	<i>n</i>	6.57	5.78	1.14 (trans)
E015	0.52	0.26	<i>n</i>	0.386	0.606	1.57 (cis)
E016	1.0	0.26	<i>n</i>	6.68	12.0	1.80 (cis)
E017b	1.0	0.33	<i>n</i>	7.32	4.84	1.51 (trans)
E018	2.0	0.76	<i>n</i>	1.10	2.05	1.86 (cis)
E019	0.60	0.20	<i>n</i>	5.52	4.43	1.25 (trans)
E020	0.44	0.16	<i>n</i>	11.6	10.3	1.13 (trans)
ESL-001-01	1.0	0.91	<i>o</i>	15.1	18.8	1.24 (cis)
<b>ESL-001-02</b>	<b>1.0</b>	<b>0.44</b>	<b>o</b>	<b>8.81</b>	<b>0.657</b>	<b>13.4 (trans)</b>
ESL-001-03	1.0	0.85	<i>o</i>	0.397	0.215	1.85 (trans)
ESL-001-04	1.0	1.0	<i>o</i>	0.128	0.0327	3.91 (trans)
ESL-001-05	1.0	0.70	<i>o</i>	1.125	0.359	3.13 (trans)
ESL-001-07	1.0	1.0	<i>o</i>	0.279	0.125	2.23 (trans)
<b>horse liver esterase</b>	<b>1.7</b>	<b>0.59</b>	<b>g</b>	<b>3.86</b>	<b>0.453</b>	<b>8.52 (trans)</b>
pig liver esterase	na	1.8	<i>i</i>	127	89.9	1.41 (trans)
pig liver esterase	0.36	0.49	<i>g</i>	23.4	11.2	2.09 (trans)
<i>Saccharomyces cerevisiae</i>	1.2	0.26	<i>g</i>	1.03	0.841	1.22 (trans)
<b>proteases</b>						
<i>Aspergillus oryzae</i>	29	7.0	<i>i</i>	0.140	0.127	1.10 (trans)
<i>Aspergillus satoii</i>	32	0.40	<i>i</i>	3.16	1.64	1.93 (trans)
<i>Bacillus licheniformis</i>	5.2	2.1	<i>g</i>	1.94	0.295	6.58 (trans)
<i>Bacillus polymyxa</i>	31	0.46	<i>i</i>	0.0876	0.0866	1.01 (trans)
<i>Bac. subtilis</i> var. <i>Biotecus</i> A	4.2	1.7	<i>g</i>	1.00	0.258	3.88 (trans)
<b>bovine pancreas</b>	<b>5.2</b>	<b>2.2</b>	<b>i</b>	<b>0.275</b>	<b>&lt;0.01</b>	<b>&gt;100 (trans)</b>
<b><math>\alpha</math>-chymotrypsin</b>	<b>5.0</b>	<b>3.0</b>	<b>i</b>	<b>0.329</b>	<b>&lt;0.01</b>	<b>&gt;100 (trans)</b>
Optimase L660	na	29	<i>p</i>	0.108	0.113	1.05 (cis)
pepsin from hog stomach	24	0.49	<i>g</i>	0.0332	0.228	6.87 (cis)
proteinase, bacterial	4.7	2.1	<i>g</i>	0.869	0.234	3.71 (trans)
proteinase K	0.42	0.066	<i>g</i>	2.64	3.04	1.15 (cis)
<i>Streptomyces caespitosus</i>	23	0.26	<i>i</i>	0.237	0.0132	18.0 (trans)

Table 1 (Continued)

source of active hydrolase <sup>a</sup>	wt <sup>b</sup>	prot <sup>c</sup>	supplier	activity		estimated D <sup>e</sup>
				trans <sup>d</sup>	cis <sup>d</sup>	
proteases (continued)						
<b>subtilisin from <i>Bacillus licheniformis</i></b>	<b>4.5</b>	<b>1.3</b>	<b>g</b>	<b>1.35</b>	<b>&lt;0.01</b>	<b>&gt;100 (trans)</b>
subtilisin Carlsberg	9.7	4.4	i	0.858	0.188	4.56 (trans)
Thermolysin, type X	2.4	0.15	i	0.281	0.186	1.51 (trans)
thrombin from human plasma	2.0	0.026	g	0.473	2.18	4.61 (cis)
acylases						
<i>Aspegillus melleus</i>	26	0.96	g	0.0519	0.0609	1.17 (cis)
hog kidney	1.1	0.71	g	0.781	0.238	3.28 (trans)

<sup>a</sup> The following hydrolases showed no detectable activity (<0.01  $\mu\text{mol}/\text{min}/\text{mg}$  protein) toward either diastereomer. Lipases: *C. antarctica* B (Novo-Nordisk), lipoprotein lipase from *C. viscosum* (Fluka), porcine pancreatic (Biocatalysts), *P. fluorescens* (Fluka); wheat germ (Sigma-Aldrich). Esterases: E012 (ThermoGen), ESL-001-06 (Diversa), *T. brockii* (Fluka). Proteases: papaya (Sigma-Aldrich), Penicillin amidase from *E. coli* (Fluka), Prolidase from *L. lactis* (Fluka), rennin from *M. meihie* (Fluka), *S. griseus* (Calbiochem/Behring), trypsin (Worthington). <sup>b</sup> Amount (mg) of solid enzyme per ml of buffer in the stock solutions. na = not available; received as a solution. <sup>c</sup> Protein concentration of stock solutions in mg protein/mL determined by the Bio-Rad assay using BSA as a standard. <sup>d</sup> Observed rate of hydrolysis in  $\mu\text{mol}/\text{min}/\text{mg}$  protein. Rates are calculated in  $\mu\text{mol}/\text{min}$  using Equation 1 then divided by the total amount of protein in each well. The values are an average of four measurements, which typically varied by less than 2%. <sup>e</sup> Ratio of the separately measured initial rates for the diastereomers. This ratio is NOT the true diastereoselectivity, but is a useful estimate. The absolute configuration of the faster reacting ester is in parentheses. <sup>f</sup> Amano Enzyme USA Co., Ltd. (Troy, VA). <sup>g</sup> Fluka Chemie (Oakville, ON). <sup>h</sup> Boehringer-Mannheim (Mannheim, Germany). <sup>i</sup> Sigma-Aldrich (Oakville, ON). <sup>j</sup> Biocatalysts Ltd. (Pontypridd, Mid Glam, Wales, UK). <sup>k</sup> Genzyme (Cambridge, MA). <sup>l</sup> Altus Biochemicals (Cambridge, Ma.). <sup>m</sup> Unilever Research Labs (Vlardingingen, The Netherlands). <sup>n</sup> ThermoGen, Inc. (Chicago, IL). <sup>o</sup> Diversa Corp. (San Diego, CA). <sup>p</sup> Genencor (Palo Alto, CA).

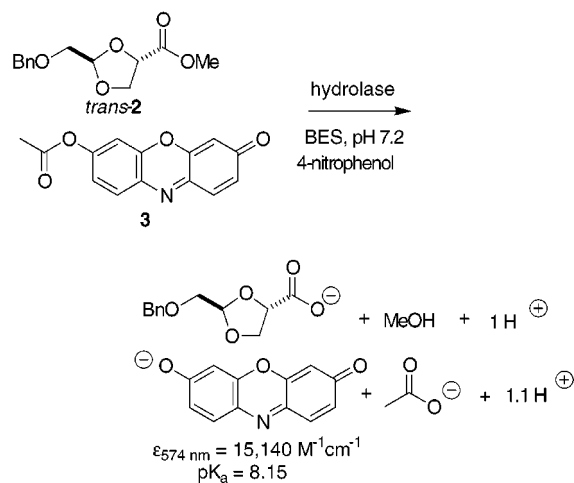


**Figure 3.** First selectivity step of a quick *D* measurement using *trans-2*. Enzyme-catalyzed hydrolysis of *trans-2* in the presence of the reference compound, resorufin acetate **3**, releases protons that produce a decrease in the yellow absorbance of the pH indicator and a brilliant pink chromophore, resorufin anion. Both of the absorbance changes, at 404 and 574 nm, respectively, can be monitored simultaneously with a microplate reader. The simultaneous initial rates of hydrolysis of each compound are calculated in  $\mu\text{mol}/\text{min}$  using eqs 2 and 3. The ratio of relative rates yields the selectivity ratio after taking into account the initial concentrations of each substrate. The second step of the quick *D* is the same, except that it uses *cis-2*. The ratio of selectivity ratios yields the diastereoselectivity, eq 4.

Figure 3. The ratio of relative rates (in  $\mu\text{mol}/\text{min}$ ) calculated using eqs 2 and 3 (see the Experimental Section), after accounting for the initial concentration of both substrates, yields the selectivity of the hydrolase,  $(k_{\text{cat}}/K_{\text{M}})_{\text{trans-2}}/(k_{\text{cat}}/K_{\text{M}})_{\text{3}}$ . The second step of the screen is the same but uses the *cis* diastereomer of **2**. Since the reference compound is the same in both experiments, the two selectivity steps can be compared and their ratio yields the true diastereoselectivity,  $(k_{\text{cat}}/K_{\text{M}})_{\text{trans-2}}/(k_{\text{cat}}/K_{\text{M}})_{\text{cis-2}}$ , eq 4 (see Experimental Section). The initial rate measurements for the two separate selectivity steps of a typical quick *D* measurement, are shown in Figure 4.

The quick *D* values for the six hydrolases were significantly lower, sometimes more than 20 times, than the estimated diastereoselectivities, Table 2. The three hydrolases with estimated diastereoselectivities >100 showed quick *D* values of only 4.4–13. Cholesterol esterase (estimated diastereoselectivity of 157) showed the highest measured quick *D* value, *D* = 17. Horse liver esterase (estimated diastereoselectivity of 8.5) showed a true diastereoselectivity of 3.5, while protease from *Streptomyces caespitosus* (estimated diastereoselectivity of 18) showed a quick *D* diastereoselectivity of 1.6.

**True Diastereoselectivity via the Endpoint Method.** To confirm that we measured the true diastereoselectivities correctly via “quick *D*” measurements, we also measured the diastereoselectivities by the traditional endpoint method (small-scale preparative reactions). Starting from a 1:1 mixture of *cis-2* and *trans-2* and using similar reaction conditions as the screening (2 mM substrate, 7% acetonitrile as cosolvent), we allowed each hydrolase to partially hydrolyze the dioxolane methyl esters. After separation of product acid from remaining ester, we measured the diastereomer composition of each by both <sup>1</sup>H NMR spectroscopy and HPLC. Diastereoselectivities from these preparative reactions agree with those measured by the quick *D* screen to within the error limits for five of the six hydrolases, Table 3. Only with horse liver esterase did the two values differ significantly –11.4 (preparative reaction) vs 3.5 (quick *D*). We attribute the lower diastereoselectivity in the quick *D* experiment to the added surfactant, Triton X-100, which was not present in preparative reactions. We previously noted a decrease in the enantioselectivity of horse liver esterase upon addition of Triton X-100.<sup>22</sup> These experiments confirm that the quick *D* method accurately measures diastereoselectivities.

**Optimization of Reaction Conditions.** We also determined the diastereoselectivities at conditions more typical of a preparative scale reaction—80 mM substrate concentration without any added acetonitrile. This reaction mixture contained droplets of undissolved substrate, and the diastereoselectivities were measured by the endpoint method, Table 3. We could not use the quick *D* method because spectrophotometric measurements re-

**Table 2.** Diastereomeric Ratios of Hydrolases toward *cis*-(2*S*,4*S*)- and *trans*-(2*R*,4*S*)-Dioxolane Methyl Esters, **2**, Using the Quick *D* Method

hydrolase <sup>a</sup>	time <sup>b</sup> (s)	<i>trans</i> -diastereomer + ref <sup>c</sup>		<i>cis</i> -diastereomer + ref <sup>c</sup>		quick <i>D</i> <sup>d</sup>	estd <i>D</i> <sup>e</sup>
		rate <sub>trans</sub>	rate <sub>ref</sub>	rate <sub>cis</sub>	rate <sub>ref</sub>		
bovine pancreatic protease	10–900	0.257	0.157	0.128	1.00	12.8 ± 2.3	> 100
cholesterol esterase	10–50	16.6	6.16	0.995	6.24	16.9 ± 4.6	157
α-chymotrypsin	10–500	0.558	0.651	0.099	0.734	6.35 ± 1.42	> 100
horse liver esterase	10–200	7.69	0.286	2.019	0.265	3.53 ± 0.6	8.5
<i>Streptomyces caespitosus</i> protease	10–900	0.289	0.0826	0.187	0.0854	1.60 ± 0.4	18
subtilisin from <i>Bacillus licheniformis</i>	10–50	4.91	9.43	1.15	9.79	4.43 ± 0.9	> 100

<sup>a</sup> See Table 1 for details. <sup>b</sup> Data collection time. <sup>c</sup> Final concentration in each well during measurement: 2.0 mM dioxolane methyl ester, 0.10 mM resorufin acetate, 0.434 mM 4-nitrophenol, 4.65 mM BES buffer, 7% acetonitrile, 0.134 mM (0.86%) Triton X-100. Changes in absorbance at 404 and 574 nm were monitored simultaneously. Rates were calculated in  $\mu\text{mol}/\text{min}$  using Equations 2 and 3. Values are in  $\mu\text{mol}/\text{min} \times 10^{-3}$ . No spontaneous chemical hydrolysis was detected. <sup>d</sup> Quick *D* calculated using eq 4. Average and standard deviation of four measurements. <sup>e</sup> Values from Table 1.

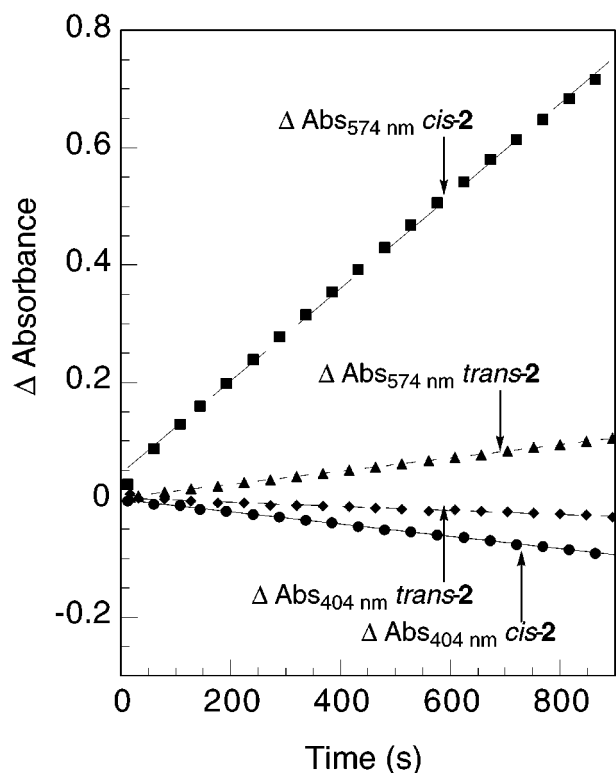


**Figure 4.** Initial rate measurements for the two selectivity steps of the quick *D* measurement with bovine pancreatic protease: one selectivity step uses *cis*-**2** and **3**, the other *trans*-**2** and **3**. The measured absorbance changes at 404 nm (accounting for the protons released from a pure diastereomer of **2** and resorufin acetate, **3**) and 574 nm (accounting for the released resorufin anion) are measured simultaneously in each selectivity experiment, and the relative initial rates of hydrolysis for each selectivity step (the selectivity ratio) are calculated using eqs 2 and 3. All initial absorbances are normalized to zero. For bovine pancreatic protease, the selectivity ratio of *trans*-**2** vs **3** is 1.64 while the selectivity ratio of *cis*-**2** vs **3** is 0.128. The ratio of the two selectivity ratios equals the diastereoselectivity, 12.8. Conditions in the well during assay: 2.0 mM *cis*- or *trans*-dioxolane methyl ester, 0.1 mM resorufin acetate, 4.65 mM BES, 0.434 mM 4-nitrophenol, 0.86% Triton X-100, 7% acetonitrile. For each initial rate measurement, points fit a straight line with a regression factor > 0.97.

quire clear solutions. Under these new conditions, the diastereoselectivity of three hydrolases did not change (cholesterol esterase, protease from *Streptomyces c.*, subtilisin), that of one hydrolase decreased (horse liver esterase), and that of two hydrolases increased by a factor

of 3.6 (α-chymotrypsin and bovine pancreatic protease). This increased selectivity make α-chymotrypsin and bovine pancreatic protease acceptable biocatalysts for the separation of *cis*-(2*S*,4*S*) and *trans*-(2*R*,4*S*) diastereomers of **2**.

To test whether this increase in diastereoselectivity arises from the increase in the substrate concentration (from **2** to 80 mM) or elimination of the acetonitrile, we also measured the diastereoselectivity of α-chymotrypsin at 80 mM substrate with 7% acetonitrile. Some substrate remained undissolved. The diastereoselectivity was an intermediate value, 16, higher than that at 2 mM substrate with 7% acetonitrile (*D* = 7.7), but lower than that at 80 mM substrate with no acetonitrile (*D* = 29). This intermediate value suggests that both the increase in substrate concentration from 2 to 80 mM and the elimination of 7% acetonitrile increase the diastereoselectivity. Other researchers have also observed decreased selectivity of α-chymotrypsin in the presence of organic solvents.<sup>25</sup>

For synthetic use, we tested the separation of a 2:1 *cis*/*trans* mixture of **2** with α-chymotrypsin because our current synthetic route to the dioxolane acids yields a 2:1 *cis*/*trans* mixture of dioxolanes. Using Sih's equation, we calculated that the desired *cis*-(2*S*,4*S*)-dioxolane methyl ester will have >98% de above 42% conversion.<sup>26</sup> We carried out the reaction at 80 mM substrate concentration, allowed the α-chymotrypsin to hydrolyze the substrate to 43% conversion, and isolated the remaining *cis*-dioxolane methyl ester in 55% yield and >98% diastereomeric excess, Figure 5.

**Computer Modeling.** Cohen developed a qualitative model to predict the enantioselectivity of α-chymotrypsin toward *N*-acylamino acid esters (e.g., *N*-acetylphenylalanine methyl ester) and related substrates.<sup>27</sup> This model, together with the X-ray structure of chymotrypsin, identified three regions that bind the acyl part of the substrate. First, and most important for tight binding, is a deep hydrophobic pocket called the specificity pocket.

(25) Neimann, C. *Science* **1964**, *143*, 1287–1296.

(26) We used the following modified form of Sih's equation for recycling, where  $de_0 = -33\%$  since the slow *cis* enantiomer is in 2:1 excess over the preferred *trans* diastereomer initially and  $de' = -98\%$  (conventional methods used for de determination have accuracies ± 2%) and used Microsoft Excel to solve the equation iteratively for conversion. See ref 21.

$$\left[1 - d\left(\frac{1 + de'}{1 + de_0}\right)\right]^E = \left[1 - d\left(\frac{1 - de'}{1 - de_0}\right)\right]^E$$

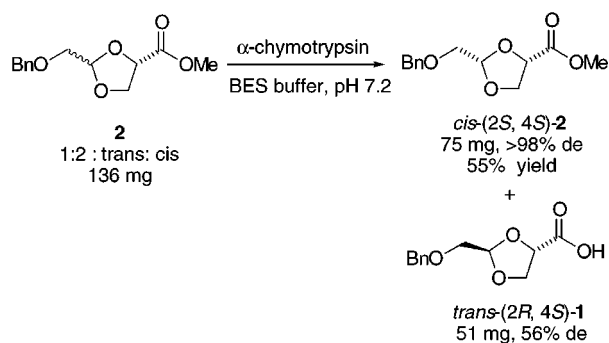
(27) Cohen, S. G. *Trans. N. Y. Acad. Sci.* **1969**, *31*, 705–719; see also ref 25.



**Table 3.** Diastereomeric Ratios of Hydrolases toward *cis*-(2*S*, 4*S*) and *trans*-(2*R*, 4*S*) Dioxolane Methyl Esters, 2, Measured by the Endpoint Method

hydrolase <sup>a</sup>	S <sup>b</sup> (mM)	time <sup>c</sup> (h)	de <sub>s</sub> <sup>d</sup> (%)	de <sub>p</sub> <sup>d</sup> (%)	C <sup>e</sup> (%)	endpoint D <sup>f</sup>	quick D <sup>g</sup>
bovine pancreatic protease	2	5.1	53.8	70.6	43.3	9.83 ± 0.3	12.8 ± 2.3
<b>bovine pancreatic protease</b>	<b>80</b>	<b>3.2</b>	<b>65.9</b>	<b>89.5</b>	<b>42.3</b>	<b>35.7 ± 3.2</b>	
cholesterol esterase	2	1.4	44.2	78.3	36.1	12.6 ± 0.53	16.9 ± 4.6
cholesterol esterase	80	2.6	68.5	69.7	49.6	11.3 ± 0.30	
α-chymotrypsin	2	3.8	42.3	67.4	38.6	7.74 ± 0.21	6.4 ± 1.4
<b>α-chymotrypsin</b>	<b>80</b>	<b>7.5</b>	<b>75.5</b>	<b>85.5</b>	<b>46.9</b>	<b>28.9 ± 1.7</b>	
horse liver esterase	2	1.5	61.0	72.2	45.8	11.4 ± 0.35	3.5 ± 0.6
horse liver esterase	80	8.0	28.7	46.2	38.3	3.56 ± 0.06	
protease from <i>Streptomyces caespitosus</i>	2	17.1	12.9	20.2	39.0	1.70 ± 0.02	1.6 ± 0.4
protease from <i>Streptomyces caespitosus</i>	80	26.2	10.9	20.0	35.3	1.66 ± 0.02	
subtilisin from <i>Bacillus licheniformis</i>	2	1.25	54.0	57.9	48.3	6.33 ± 0.13	4.4 ± 0.9
subtilisin from <i>Bacillus licheniformis</i>	80	4.5	58.8	55.1	51.6	6.10 ± 0.11	

<sup>a</sup> See Table 1 for details. <sup>b</sup> Substrate concentration in the reaction mixture. <sup>c</sup> Reaction time. <sup>d</sup> Measured diastereomeric excess of the remaining starting material (de<sub>s</sub>) or product acid (de<sub>p</sub>). <sup>e</sup> Degree of conversion calculated by de<sub>s</sub>/(de<sub>s</sub> + de<sub>p</sub>). <sup>f</sup> The diastereoselectivity was calculated from de<sub>s</sub> and de<sub>p</sub> as defined by: Chen, C. S.; Fujimoto, Y.; Girdaukas, G.; Sih, C. J. *J. Am. Chem. Soc.* **1982**, *104*, 7294–7299. The *trans* diastereomer was preferentially hydrolyzed in all cases. Error limits on diastereoselectivities were calculated using an estimated 1% maximum error in integration since the diastereomers were separated with baseline resolution. <sup>g</sup> Values from Table 2.

**Figure 5.** Preparative-scale separation of a 1:2 *trans*/*cis* mixture of **2** using α-chymotrypsin.

This specificity pocket accounts for α-chymotrypsin's preference for amides and esters of amino acids with aromatic side chains, e.g., phenylalanine.<sup>28</sup> Second is a polar site called the *am*-site (amide site) that favors the *N*-acyl group. This site contains a hydrogen bond acceptor, the carbonyl oxygen of Ser 214. Third is a small site called the *h*-site (hydrogen site). This model is too qualitative to explain the diastereoselectivity of α-chymotrypsin toward dioxolanes, **2**, because their structures differ significantly from *N*-acylamino acid esters. In particular, the stereocenter in dioxolanes lies three bonds away from the reacting carbonyl group, while in *N*-acylamino acid esters the stereocenter lies one bond away (a γ- instead of an α-stereocenter).

To rationalize the high diastereoselectivity of α-chymotrypsin toward the dioxolanes, **2**, we used computer modeling of enzyme–transition-state analogue complexes. Since α-chymotrypsin is a serine protease, the first step in an ester hydrolysis is the attack of the O<sub>γ</sub> of the active site serine at the ester carbonyl forming a tetrahedral intermediate.<sup>29</sup> Collapse of this tetrahedral intermediate releases the alcohol. We assume that the transition state involved in formation or collapse of this first tetrahedral intermediate defines the selectivity of α-chymotrypsin toward dioxolanes, **2**. To mimic this transition state, we used the phosphonates linked to α-chymotrypsin shown in Figure 6a. Indeed, researchers

have shown that phosphonates mimic well the transition state for ester hydrolysis.<sup>30</sup>

To position the phosphonate covalently to the O<sub>γ</sub> of serine 195. To position the dioxolane ring, we considered all three possible staggered conformations along the phosphorus–carbon bond. This gave three conformations for *cis*-**2a–c** and for *trans*-**2a–c**. The three different staggered conformations place the hydrogen (conformation a), the methylene (conformation b), or the oxygen (conformation c) in the polar *am*-site. For each conformation, we manually adjusted the orientation of the benzyl moiety so that it fit into α-chymotrypsin's specificity pocket. The binding of hydrophobic groups to this pocket is the strongest substrate–chymotrypsin interaction, so we assumed that the benzyl group binds in this pocket.

We assumed that a catalytically productive complex required all five hydrogen bonds within the catalytic machinery shown in Figure 6a. We set generous limits for a hydrogen bond: a donor to acceptor atom distance of less than 3.1 Å with a nearly linear arrangement (>120° angle) of donor atom, hydrogen, and acceptor atom. Structures lacking two or more of the five hydrogen bonds were nonproductive. However, structures lacking only one hydrogen bond may be productive if the hydrogen bond is only slightly outside the limits set above. The two lowest energy structures for the *trans* isomer (*trans*-**2c** and **-2b**) are possibly productive, Table 4, because one or two hydrogen bonds are weak. On the other hand, the lowest energy structures for the *cis* isomer (*cis*-**2a** and **-2b**) are not productive because the hydrogen bonds are significantly too long. Figure 6b,c shows the lowest energy structures (*trans*-**2c** and *cis*-**2a**).

This modeling suggests that the *cis* diastereomer binds tightly, but in a nonproductive orientation,<sup>31</sup> because the lowest energy structures for the *cis* diastereomer are nonproductive. On the other hand, the lowest energy structure for the *trans* diastereomer is slightly higher in energy, but productive, suggesting this isomer binds less tightly, but binds in a reactive conformation.

(30) Phosphonates strongly inhibit hydrolases; for example: Hanson, J. E.; Kaplan, A. P.; Bartlett, P. A. *Biochemistry* **1989**, *28*, 6294–6305. Antibodies to phosphonates often catalyze hydrolysis of the corresponding esters; for example: Jacobs, J.; Schultz, P. G.; Sugawara, R.; Powell, M. *J. Am. Chem. Soc.* **1987**, *109*, 2174–2176.

(31) We were unable to accurately determine the *K<sub>M</sub>* values for *cis*-**2** and *trans*-**2** since both *K<sub>M</sub>* values were above 4 mM, the solubility limit of both diastereomers under our reaction conditions.

(28) Kundu, N.; Roy, S.; Maenza, F. *Eur. J. Biochem.* **1972**, *28*, 311–315.

(29) Branden, C.; Tooze, J. *Introduction to Protein Structure*; Garland: New York, 1991; pp 231–246.

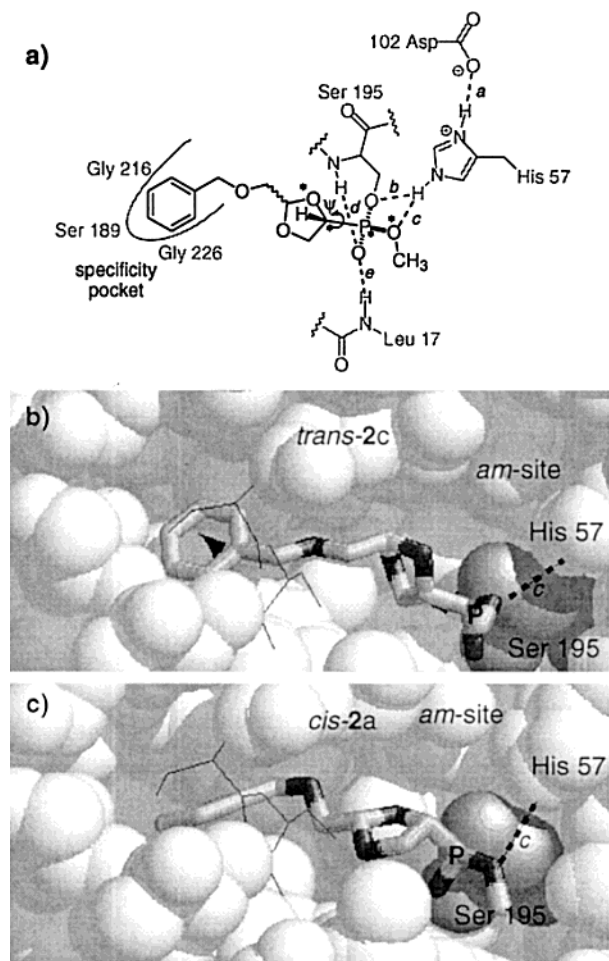


**Figure 6.** Transition-state analogues for the  $\alpha$ -chymotrypsin-catalyzed hydrolysis of dioxolane esters *trans*- and *cis*-**2**. (a) Line diagram. The  $O_\gamma$  of the catalytic serine (Ser 195) attacks the ester carbonyl forming a tetrahedral intermediate. The phosphonate above (black lines) mimics this tetrahedral intermediate.  $\alpha$ -Chymotrypsin residues are drawn in gray. Five hydrogen bonds, marked *a*–*e*, stabilize the charges. To be judged catalytically competent, the minimized structures must contain all five hydrogen bonds. Three conformations for each dioxolane were constructed by varying the torsion angle marked  $\psi$  and defined by the atoms marked with asterisks. For each conformation, the phenyl ring was fit into the hydrophobic pocket manually. (b) Lowest energy conformation for the phosphonate transition state analogue of *trans*-**2** (sticks representation) in the active site of  $\alpha$ -chymotrypsin (space filling). To expose the specificity pocket, two amino acid residues—Ser217 and Ser218—are shown in line representation. Dark gray indicates the oxygen atoms of the transition state analogue, and a 'P' indicates the phosphorus. Labels indicate the catalytic serine (gray) and histidine (not highlighted). Hydrogen atoms and water molecules are hidden for clarity. A dioxolane oxygen points toward the polar region of the active site, formed by the carbonyl oxygen of Ser 124 (marked *am*-site). A dashed line labeled *c* indicates a key hydrogen bond between oxygen of the OMe and His 57. In this structure, this hydrogen bond is present, but weak, suggesting that this is a catalytically competent structure. (c) Lowest energy conformation for the phosphonate transition-state analogue for *cis*-**2** labeled as in b. A dioxolane C–H points toward the polar region of the active site, formed by the carbonyl oxygen of Ser 124 (marked *am*-site). A dashed line labeled *c* marks a key hydrogen bond between oxygen of the OMe and His 57. In this structure, this hydrogen bond is too long, suggesting that this is a nonproductive structure.

## Discussion

Extending two previously developed screening methods for activity and enantioselectivity to measure diastereoselectivity, we rapidly identified two active and selective proteases,  $\alpha$ -chymotrypsin from bovine pancreas and bovine pancreatic protease, useful for the separation of diastereomeric mixtures of *cis*-(2*S*,4*S*)- and *trans*-(2*R*,4*S*)-dioxolane methyl esters. We then optimized the  $\alpha$ -chymotrypsin-catalyzed separation of a 2:1 *cis*/*trans* mixture of the dioxolane methyl ester, **2**, to yield the *cis*-(2*S*,4*S*)-dioxolane methyl ester in high de (>98%) and good yield (55% overall from a 2:1 *cis*/*trans* mixture). This enzymatic separation simplifies the preparation of a key intermediate in the synthesis of dioxolane nucleosides.

We previously reported that screening for estimated *E* with separate enantiomers estimated the enantioselectivities of a library of hydrolases toward solketal butyrate.<sup>22</sup> Other researchers have also used the initial rates of hydrolysis of pure enantiomers to estimate enantioselectivity.<sup>32</sup> However, we found the separately measuring the initial rates of hydrolysis of the pure diastereomers of **2** overestimated the diastereoselectivities by as much as 20-fold. Only one of six estimated *D* values agreed with the true diastereoselectivities determined by the endpoint method. We attribute this difference to differences in  $K_M$  values between the two diastereomers that are ignored in the estimated *D* screen. The large benzyl protecting group strongly prefers to bind in the  $S_1$  pocket in  $\alpha$ -chymotrypsin and our molecular modeling studies suggest that, to bind the benzyl group in this site, the *cis* diastereomer binds in a tight, nonproductive conformation while the *trans* diastereomer binds in a less tight but productive conformation.

When we measure initial rates of hydrolysis of the diastereomers separately in the screen for estimated *D*, we eliminate competitive binding between the two diastereomers in the enzyme active site, thereby ignoring some or all of the contributions of  $K_M$  to the diastereoselectivity.<sup>23</sup> Introduction of a reference compound in quick *D* reintroduces competition to the assay. When multiple substrates compete for the enzyme active site (in this case, a pure diastereomer of **2** and resorufin acetate, **3**), the ratio of their initial rates of hydrolysis, after taking into account their initial concentrations, equals their relative  $k_{cat}/K_M$  values.<sup>33</sup> The ratio of the two selectivity experiments yields the diastereoselectivity. Researchers have previously measured the initial rates of hydrolysis of mixtures of peptides to determine relative  $k_{cat}/K_M$  values for proteases.<sup>34</sup>

The two most selective hydrolases identified by our screening methods were both proteases isolated from bovine pancreas and may indeed be the same enzymes. Although bovine pancreatic protease (Sigma) is a crude preparation while  $\alpha$ -chymotrypsin (Sigma) is a purified protein, both had similar activity toward 4-nitrophenyl acetate and both had essentially the similar protein

(32) Reetz, M. T.; Zonta, A.; Schimossek, K.; Liebeton, K.; Jaeger, K.-E. *Angew. Chem., Int. Ed. Engl.* **1997**, *36*, 2830–2832. Kitaguchi, H.; Fitzpatrick, P. A.; Huber, J. E.; Klivanov, A. M. *J. Am. Chem. Soc.* **1989**, *111*, 3094–3095.

(33) For a discussion of multiple substrate kinetics, see: Schellenberger, V.; Siegel, R. A.; Rutter, W. J. *Biochemistry* **1993**, *32*, 4344–4348.

(34) Bermann, J.; Green, M.; Sugg, E.; Anderegg, R.; Millington, D. S.; Norwood, D. L.; McGeehan, J.; Wiseman, J. *J. Biol. Chem.* **1992**, *267*, 1434–1437.



**Table 4. Minimized Structures for the Transition-State Analogues for the  $\alpha$ -chymotrypsin-Catalyzed Hydrolysis of Dioxolane Esters *trans-2* and *cis-2***

conformation	$\psi^a$ (deg)	group in <i>am-site</i> <sup>b</sup>	H-bond c distance <sup>c</sup> (Å) (N–H–O angle, deg)	steric energy, <sup>d</sup> kcal/mol	comments
<i>trans-2c</i>	61	O	3.55 (154)	1.1	possibly productive, H-bond <i>b</i> is also weak: 3.40 Å, 142°
<i>trans-2b</i>	–64	CH <sub>2</sub>	3.67 (161)	2.7	possibly productive
<i>trans-2a</i>	–177	H	4.25 (164)	6.8	not productive
<i>cis-2a</i>	–179	H	3.99 (157)	0	not productive
<i>cis-2b</i>	–62	CH <sub>2</sub>	3.80 (152)	2.7	unlikely productive
<i>cis-2c</i>	59	O	3.22 (143)	6.7	possibly productive, H-bond <i>d</i> between amide NH of Ser 195 and phosphoryl oxygen is very weak: 3.65 Å, 140°

<sup>a</sup> Dihedral angle along the phosphorus–carbon bond as defined by the asterisks in Figure 6a. <sup>b</sup> When *N*-acylamino acid esters or amide bind to the active site of  $\alpha$ -chymotrypsin, the *N*-acyl group binds in a polar region containing a hydrogen bond acceptor, the carbonyl oxygen of Ser 214. The part of the dioxolane that binds in this region is indicated. <sup>c</sup> See Figure 6a for the definitions of the hydrogen bonds. Unless otherwise noted, hydrogen bonds *a*, *b*, *d*, and *e* (His 57 to Aps 102, amide NH of Ser 195 to the phosphoryl oxygen, and amide NH of Leu 17 to the phosphoryl oxygen) were present (N–O distance 2.8–3.1 Å, N–H–O angle 130–170°) in all structures. <sup>d</sup> Energies are relative to the lowest energy of the six structures.

content, 30 and 32 wt % protein/wt % solid, respectively. Both had similar activity in the scale-up reactions with 80 mM substrate (2.4 U/mg protein for  $\alpha$ -chymotrypsin, 1.8 U/mg protein for bovine pancreatic protease) and in screening reactions toward 2 mM *trans-2* (0.329  $\mu$ mol/min/mg protein for  $\alpha$ -chymotrypsin; 0.275  $\mu$ mol/min/mg for bovine pancreatic protease). The initial rates toward *cis-2* were too slow to measure for both hydrolases. These similar activities and diastereoselectivities suggest that  $\alpha$ -chymotrypsin is present in commercial bovine pancreatic protease and may be responsible for the observed activity and diastereoselectivity. Both hydrolases are also similar in cost ( $\alpha$ -chymotrypsin = \$0.55/U toward a 2:1 *cis/trans* mixture of **2**, bovine pancreatic pancreas = \$0.42/U) so either is useful for preparative scale separations.<sup>35</sup>

Other groups have also separated diastereomers by selective hydrolysis of their ester derivatives.<sup>36</sup> Examples most similar to those in this paper are the separation of *cis* and *trans* isomers in three- or six-membered rings. In three-membered rings, Schneider et al. separated *cis* and *trans* isomers of chrysanthemide and related acids using pig liver esterase.<sup>37</sup> In six-membered rings, Königsberger et al. separated *cis*- and *trans*-4-substituted cyclohexanecarboxylates using lipase from *Candida rugosa*,<sup>38</sup> while Ogasawara and co-workers separated *cis*- and *trans*-4-*tert*-butylcyclohexanemethanols and 1,4-cyclohexanedimethanol using lipase from *Pseudomonas cepacia* (PCL).<sup>39,40</sup> In each case, the esterase or lipase favored the *trans* isomer with moderate to excellent diastereoselectivity. The dioxolanes in this paper are five-membered rings. Stereoisomers within five-membered rings are more difficult to separate because they are flexible and adopt several conformations. 1,3-Dioxolane rings are

flexible even with bulky alkyl substituents at the 2- and 4-positions.<sup>41</sup> In contrast, stereoisomers in three- and six-membered rings are rigid and thus usually easier to separate than those in five-membered rings. Wang and co-workers recently separated diastereomers of the nucleoside analogues,  $\alpha$ -L-taluronamide and  $\beta$ -D-alluronamide using hydrolases.<sup>42</sup> The stereochemistry within the ribose ring was fixed, and the diastereomers differed in the stereochemistry at a secondary hydroxyl group in the side chain. Reaction occurred at this secondary hydroxyl group. Our separation differs because it involved a stereocenter within the ring, the stereocenter was three bonds away from the point of hydrolysis, and the stereocenter was in the acyl part of an ester instead of alcohol part.

In summary, an extension of our enantioselectivity screen to diastereoselectivity screening identified two useful hydrolases that simplify preparation of intermediates for the synthesis of antiviral and anticancer drugs.

## Experimental Section

**General Methods.** Chemicals were purchased from Sigma-Aldrich Co. (Oakville, ON) and were used without further purification unless stated. Enzyme suppliers are noted in the footnotes of Table 1. Polystyrene 96-well flat-bottomed microplates (maximum volume 360  $\mu$ L/well) were filled using eight-channel pipets (5–100  $\mu$ L, 50–1200  $\mu$ L) and solution basins for multichannel pipets. Melting points are corrected values. The diagrams in Figure 6b,c were drawn with RasMac v. 2.6.<sup>43</sup>

**2-(*R,S*)-benzyloxymethyl-4(*S*)-carboxylic Acid 1,3-Dioxolane Methyl Esters, **2**.** The preparation of (2*S*,4*S*)-*cis*- and (2*R*,4*S*)-*trans*-dioxolane acids, **1**, were previously described in the literature.<sup>8,9</sup> We prepared the diastereomers of **1** starting from benzyloxyacetaldehyde and 2,3-*O*-isopropylidene-(*S*)-glyceric acid methyl ester<sup>10</sup> following a procedure by Norbeck et al.<sup>2a</sup> The mixture of *cis* and *trans* esters was hydrolyzed to the corresponding acids for separation by silica gel chromatography using 99/0.5/0.5 dichloromethane/methanol/acetic acid as eluent, since we were unable to find conditions suitable for separation of diastereomers of **2**. The pure diastereomers were then converted back to methyl esters using dimethoxypropane and catalytic HCl.<sup>44</sup> <sup>1</sup>H NMR and <sup>13</sup>C NMR are

(35) Cost per unit ( $\mu$ mol of substrate hydrolyzed per minute) is calculated using commercial prices listed by Sigma-Aldrich Canada Ltd., 1998.

(36) Schirmeister, T.; Otto, H.-H. *J. Org. Chem.* **1993**, *58*, 4819–4822. Levayer, F.; Rabiller, C.; Tellier, C. *Tetrahedron: Asymmetry* **1995**, *6*, 1675–1682. Morgan, B.; Stockwell, B. R.; Dodds, D. R.; Andrews, D. R.; Sudhakar, A. R.; Nielson, C. M.; Mergelsberg, I.; Zumbach, A. *JAOCS* **1997**, *74*, 1361–1370. Angelis, Y. S.; Smonou, I. *Tetrahedron Lett.* **1998**, *39*, 2823–2826.

(37) Schneider, M.; Engel, N.; Boensmann, H. *Angew. Chem., Int. Ed. Engl.* **1984**, *23*, 64–66.

(38) Königsberger, K.; Luna, H.; Prasad, K.; Repic, O.; Blacklock, T. J. *Tetrahedron Lett.* **1996**, *37*, 9029–9032.

(39) Hiroya, K.; Hasegawa, J.; Watanabe, T.; Ogasawara, K. *Synthesis* **1995**, 379–381.

(40) Watanabe, T.; Hasegawa, J.; Hiroya, K.; Ogasawara, K. *Chem. Pharm. Bull.* **1995**, *43*, 529–531.

(41) Willy, W. E.; Binsch, G.; Eliel, E. L. *J. Am. Chem. Soc.* **1970**, *92*, 5394–5402.

(42) Wang, J.-Q.; Archer, C.; Li, J.; Bott, S. G.; Wang, P. G. *J. Org. Chem.* **1998**, *63*, 4850–4853.

(43) Sayle, R. A.; Milner-White, E. J. *Trends Biochem. Sci.* **1995**, *20*, 374–376.

(44) Rachele, J. R. *J. Org. Chem.* **1963**, *28*, 2898.

provided because the literature references did not include NMR data of the methyl esters.

**2(*R*)-Benzyloxymethyl-4(*S*)-carboxylic acid 1,3-dioxolane methyl ester (*cis*-2):** clear oil; 99.6% de by HPLC;  $^1\text{H}$  NMR ( $\text{CDCl}_3$ , 400 MHz)  $\delta$  3.56–3.65 (m, 2H), 3.78 (s, 3H), 3.99 (dd, 1H,  $J = 8.2$  Hz, 5.4 Hz), 4.31 (dd, 1H,  $J = 8.2$  Hz, 11.8 Hz), 4.66 (dd, 1H,  $J = 7.1$  Hz, 6.3 Hz), 4.69 (s, 2H), 5.33 (t, 1H,  $J = 4.6$  Hz), 7.27–7.35 (m, 5H);  $^{13}\text{C}$  NMR ( $\text{CDCl}_3$ , 400 MHz)  $\delta$  51.4, 67.2, 69.2, 72.7, 73.0, 103.3, 125.7, 126.8, 127.4, 136.8, 170.3.

**2(*S*)-Benzyloxymethyl-4(*S*)-carboxylic acid 1,3-dioxolane methyl ester (*trans*-2):** clear oil; 98.7% de by HPLC;  $^1\text{H}$  NMR ( $\text{CDCl}_3$ , 400 MHz) 3.63–3.72 (m, 2H), 3.74 (s, 3H), 4.10 (dd, 1H,  $J = 8.6$  Hz, 7.5 Hz), 4.25 (dd, 1H,  $J = 8.7$  Hz, 3.8 Hz), 4.60 (dd, 1H,  $J = 7.3$  Hz, 3.8 Hz), 4.63 (s, 2H), 5.23 (t, 1H,  $J = 4.6$  Hz), 7.27–7.37 (m, 5H);  $^{13}\text{C}$  NMR ( $\text{CDCl}_3$ , 400 MHz)  $\delta$  51.4, 67.5, 69.8, 72.7, 72.8, 103.8, 125.3, 125.8, 127.4, 135.9, 170.0.

**Resorufin Acetate, 3.** This compound was prepared using a modified procedure by Kramer and Guilbault.<sup>45</sup> To a slurry of resorufin sodium salt (95% purity, 1.02 g, 4.32 mmol) in 60 mL of anhydrous dichloromethane was added anhydrous pyridine (0.349 mL, 4.32 mmol, 1 equiv). The mixture was cooled in an ice bath, and then acetyl chloride (0.614 mL, 8.63 mmol, 2 equiv) was added dropwise over 10 min. The deep purple reaction mixture immediately turned orange upon addition of acetyl chloride. The reaction was warmed to room temperature and stirred overnight. The reaction was diluted with dichloromethane to 300 mL and filtered through a coarse glass frit to remove unreacted resorufin, and the solvent was removed in vacuo. The reddish-orange residue was recrystallized from ethanol, yielding a crimson powder, 0.48 g (1.89 mmol, 44% yield):  $R_f = 0.20$  (2:1, hexanes/ethyl acetate); mp = 217–220 °C (sample darkens at 215 °C) [lit.<sup>45</sup> mp = 223–225 °C (uncorrected)]; the  $^1\text{H}$  NMR spectrum matches that reported previously;<sup>46</sup>  $^{13}\text{C}$  NMR ( $d_6$ -DMSO, 200 MHz)  $\delta$  22.2, 106.3, 110.1, 119.7, 130.8, 130.9, 134.6, 135.0, 143.8, 147.9, 149.2, 152.9, 168.2, 184.9; MS (EI)  $m/z$  255 ( $\text{M}^+$ , 14), 213 (100), 185 (72), 156 (7), 128 (4), 63 (14), 43 (9); HRMS (EI) calcd for  $\text{C}_{14}\text{H}_9\text{N}_1\text{O}_4$  255.0532, found 255.0533, 0.6 ppm error.

**Hydrolase Library.** Since most hydrolases have maximal activity near neutral pH 7, we screened all hydrolases at pH 7.2. Previously, we optimized our pH indicator assay for neutral pH.<sup>22</sup> The hydrolases were dissolved in BES buffer (5.0 mM, pH 7.2 containing 0.02%  $\text{NaN}_3$  as preservative) at the concentrations listed in Table 1 (0.26–86 mg solid/mL solution).  $\text{CaCl}_2$  (2 mM) was added to the protease solutions since some proteases require calcium ions to maintain their structure. For crude samples of hydrolase, we used saturated solutions (up to 86 mg solid/mL), but for purified hydrolases, we chose lower concentrations (typically 1 mg solid/mL). Each solution was centrifuged to remove insoluble material (5 min, 2000 rpm) and titrated to a final pH of 7.2. The protein concentrations were determined using a dye-binding assay from Bio-Rad (Mississauga, ON) with bovine serum albumin (BSA) as the standard. Solutions were stored in a 96-well assay block “mother plate” equipped with aluminum sealing tape (2 mL maximum volume in each well, Corning Costar, Acton, MA) at –20 °C. This mother plate speeds up repeated screens using the same hydrolases and is a convenient way to store large libraries of hydrolases. Hydrolytic activity of the libraries is maintained over several months.

**Estimated Diastereoselectivity.** The assay solutions were prepared by mixing *cis*- or *trans*-2 (504  $\mu\text{L}$  of a 50.0 mM solution in acetonitrile), acetonitrile (386  $\mu\text{L}$ ), 4-nitrophenol (6,000  $\mu\text{L}$  of a 0.9115 mM solution in 5.0 mM BES, pH 7.2), and BES buffer (5,110  $\mu\text{L}$  of a 5.0 mM solution, pH 7.2). This solution was vortexed to ensure complete mixing. Hydrolase solutions (5  $\mu\text{L}$ /well) were transferred from the mother plate to a 96-well microplate using an eight-channel pipet. Assay solution (100  $\mu\text{L}$ /well) was added to each well using a 1,200

$\mu\text{L}$  eight-channel pipet. The final concentrations in each well were 2.0 mM substrate, 4.65 mM BES, 0.430 mM 4-nitrophenol, 7.1% acetonitrile. The plate was quickly placed in the microplate reader and shaken for 10 s to ensure complete mixing, and the decrease in absorbance at 404 nm was monitored at 25 °C as often as permitted by the microplate software, typically every 11 s. The starting absorbance was typically 1.2. Data were collected for 20 min to ensure we detected slow reactions and reactions with a lag time. Each hydrolysis was carried out in quadruplicate and was averaged. The first 10 s of data were sometimes erratic, possibly due to dissipation of bubbles created during shaking. For this reason, we typically excluded the first 10 s of data from the calculation of the initial rate. Activities were calculated from slopes in the linear portion of the curve usually over the first two hundred seconds. The initial rates were calculated from the average  $dA/dt$ , using eq 1 where  $\Delta\epsilon = 17\,300\text{ M}^{-1}\text{ cm}^{-1}$  (accounting for the fully deprotonated and protonated forms of the pH indicator, experimentally determined for our conditions) and  $l = 0.306\text{ cm}$ . To calculate specific activity ( $\mu\text{mol}/\text{min}/\text{mg}$  protein), we took into account the total amount of protein in each well.

$$\text{rate} = \frac{dA_{404\text{nm}}}{dt} \times \frac{[\text{buffer}]}{[\text{indicator}]} \times \frac{1}{\Delta\epsilon_{404\text{nm}} \cdot l} \times \text{reaction volume} \times 10^6 \quad (1)$$

**True Diastereoselectivity Using Quick D.** The assay solutions were prepared by mixing 4-nitrophenol (6000  $\mu\text{L}$  of a 0.9115 mM solution in 5.0 mM BES, pH 7.2), BES buffer (5120  $\mu\text{L}$  of a 5.0 mM solution containing 0.33 mM (2.11%) Triton X-100, pH 7.2), and acetonitrile (41.6  $\mu\text{L}$ ) and then vortexing the solution. *cis*- or *trans*-2 (90.4  $\mu\text{L}$  of a 279 mM solution in acetonitrile) and resorufin acetate, 3 (748  $\mu\text{L}$  of a 1.69 mM solution in acetonitrile; note that the solubility limit of resorufin acetate in acetonitrile is  $\sim 2$  mM) were added dropwise to the slowly vortexing solution to ensure the formation of micelles and clear solutions. Hydrolase solutions (5  $\mu\text{L}$ /well) were transferred from the mother plate to a 96-well microplate using an eight-channel pipet. Assay solution (100  $\mu\text{L}$ /well) was added to each well using a 1,200  $\mu\text{L}$  eight-channel pipet. The final concentrations in each well were 2.0 mM dioxolane methyl ester, 0.10 mM resorufin acetate, 4.65 mM BES, 0.434 mM 4-nitrophenol, 0.134 mM (0.86%) Triton-X100, 7% acetonitrile. The plate was quickly placed in the microplate reader and shaken for 10 s to ensure complete mixing, and the simultaneous decrease in absorbance at 404 nm and increase in absorbance at 574 nm were monitored at 25 °C as often as permitted by the microplate software, typically every 17 s. Data were collected for 20 min. Each hydrolysis was carried out in quadruplicate and was averaged. The first 10 s of data were sometimes erratic, possibly due to dissipation of bubbles created during shaking. For this reason, we excluded the first 10 s of data from the calculation of the initial rate. This procedure was repeated for the other enantiomer with the reference compound. Rates of hydrolysis in  $\mu\text{mol}/\text{min}$  were calculated using eqs 2 and 3 from slopes of the linear, initial portion of the curve where  $\Delta\epsilon_{404} = 17\,300\text{ M}^{-1}\text{ cm}^{-1}$  and  $\epsilon_{574} = 15\,140\text{ M}^{-1}\text{ cm}^{-1}$  (experimentally determined for our conditions) and  $l = 0.306\text{ cm}$ .

$$\text{rate}_3 = \frac{dA_{574\text{nm}}}{dt} \times \frac{1}{\epsilon_{574} \cdot l} \times \text{reaction volume} \times 10^6 \quad (2)$$

$$\text{rate}_{\text{cis-2 or trans-2}} = \left[ \frac{dA_{404\text{nm}}}{dt} \times \frac{[\text{buffer}]}{[\text{indicator}]} \times \frac{1}{\Delta\epsilon_{404\text{nm}} \cdot l} \times \text{reaction volume} \times 10^6 \right] - 1.1 \times [\text{rate}_3] \quad (3)$$

(45) Kramer, D. N.; Guilbault, G. G. *Anal. Chem.* **1964**, *36*, 1662–1663.

(46) Kitson, T. M. *Bioorg. Chem.* **1996**, *24*, 331–339.

For very active hydrolases, we used the slope over the first 50 s, but for less active hydrolases, we used up to the first 900 s. The quick *D* value was calculated from the ratio of initial



rates from the two screening steps, after taking into account the initial concentrations of the substrates, eq 4.

$$\text{quick } D = \frac{\text{trans selectivity step}}{\text{cis selectivity step}} = \frac{\text{rate}_{\text{trans-2}}}{\text{rate}_3} \times \frac{[\text{3}]}{[\text{trans-2}]} \bigg/ \frac{\text{rate}_{\text{cis-2}}}{\text{rate}_3} \times \frac{[\text{3}]}{[\text{cis-2}]} \quad (4)$$

**True Diastereoselectivity Using Small-Scale Reactions.** The reaction conditions mimic those in the microplate during estimated diastereoselectivity except that the pH indicator, reference compound, and Triton X-100 are not present. Hydrolase solutions (500  $\mu\text{L}$ ) were added to solutions of 1:1 *cis/trans*-2 (3.5 mL of a 28.8 mM in acetonitrile) and BES buffer (46 mL of a 5.0 mM solution, pH 7.2) for a final reaction volume of 50 mL (2.0 mM substrate, 4.65 mM BES, 7% acetonitrile). The final solutions were clear. The rates of hydrolysis were monitored by pH-stat, which maintained the pH at 7.2 by automatic titration with 0.0981 N NaOH. Reactions were stopped when the pH-stat indicated ~40% conversion by extracting the starting ester with ethyl acetate (3  $\times$  20 mL). The aqueous layer was adjusted to pH 2 with 1 N HCl and the dioxolane acid extracted with ethyl acetate (3  $\times$  20 mL). Ethanol was added dropwise during the workups when necessary to break up emulsions. Both extracts were dried with  $\text{MgSO}_4$ , filtered, and concentrated in vacuo. The diastereomeric excesses were measured as described below, and the diastereomeric ratio, *D*, was calculated according to Sih.<sup>21</sup> There was no detectable chemical hydrolysis of the substrate at pH 7.2. We did not observe any diastereomer enrichment or epimerization of the substrate or product during workup.

**Scale-Up Reactions with 80 mM Substrate.** Hydrolase solution (500  $\mu\text{L}$ ) was added to a solution of 1:1 *cis/trans*-2 (212 mg) and BES buffer (9,800  $\mu\text{L}$  of a 5.0 mM solution, pH 7.2) for a final reaction volume of 10.5 mL (80.0 mM substrate, 4.9 mM BES). The substrate was present as oil droplets. Reactions were carried out and worked up as above.

**Determination of Diastereomeric Purity by NMR.** Analysis was performed on a Varian Gemini 200 MHz NMR spectrometer in  $\text{CDCl}_3$ . The C2-H in the trans ester shows a triplet at  $\delta$  5.33 ( $^3J = 4.6$  Hz), and the C2-H in the cis ester shows a triplet upfield at  $\delta$  5.23 ( $^3J = 4.6$  Hz). The C2-H in the trans acid shows a triplet at  $\delta$  5.33 ( $^3J = 3.6$  Hz), while the C2-H in the cis acid shows a broad singlet upfield at  $\delta$  5.19.

**Determination of Diastereomeric Purity by HPLC.** To further confirm the diastereomeric excesses determined by NMR, we also determined diastereomeric excesses using HPLC. Diastereomeric excesses agreed well, typically <1% variation between values determined by NMR and HPLC. Diastereomers of the dioxolane acids were analyzed using a YMC ODS-AM 5  $\mu\text{m}$ , 120 A, 4.6 mm i.d.  $\times$  250 mm column (YMC, Wilmington, N.C.) and a Waters in-line precolumn filter kit. The mobile phase was composed of  $\text{H}_2\text{O} + 0.01\%$  TFA, pH 3.28 (pH was adjusted using 5 N NaOH) and  $\text{CH}_3\text{CN} + 0.01\%$  TFA. A gradient was run from 30%  $\text{CH}_3\text{CN}$  to 55%  $\text{CH}_3\text{CN}$  over 50 min with a flow rate of 0.5 mL/min. The detector was set at 210 nm:  $K_{\text{trans}} = 3.21$ ,  $K_{\text{cis}} = 3.52$ ,  $\alpha = 1.10$ ,  $R_s = 1.33$ . The same HPLC system was used to analyze the diastereomers of the dioxolane methyl esters but we used Millennium 32 Version 3.00 software and a Phenomenex Prodigy ODS 3  $\mu\text{m}$  100 A 4.6 mm i.d.  $\times$  250 mm column (Phenomenex, Torrance, CA) with a Waters in-line precolumn filter kit. The composition of the mobile phase was isocratic 25%  $\text{CH}_3\text{CN} + 0.01\%$  TFA and 75%  $\text{H}_2\text{O} + 0.01\%$  TFA, pH 3.28. The flow rate was 1.0 mL/min, and the detector was set at 200 nm:  $K_{\text{cis}} = 23.6$ ,  $K_{\text{trans}} = 24.9$ ,  $\alpha = 1.05$ ,  $R_s = 2.5$ .

**Enzyme-Catalyzed Synthesis of *cis*-(2*S*,4*S*)-Dioxolane Methyl Ester.** A 2:1 mixture of *cis/trans*-2 (136.5 mg, 0.541 mmol) was weighed into a reaction vessel, and BES buffer (6,263  $\mu\text{L}$  of a 5 mM solution, pH 7.2) was added. The substrate remained as insoluble droplets.  $\alpha$ -Chymotrypsin<sup>47</sup> (500  $\mu\text{L}$ , 0.019 units by PNPA assay) was added to begin the reaction, and the rate and degree of hydrolysis was monitored by a pH-stat that maintained the pH at 7.2 by automatic titration with 0.0981 N NaOH. The reaction was stopped at 43% conversion by extracting the remaining starting material ester with ethyl acetate (3  $\times$  20 mL). Sih's equations for recycling<sup>26</sup> predict that this degree of conversion would give high diastereomeric purity for the remaining starting material. The aqueous layer was adjusted to pH 2, and the product acid extracted with ethyl acetate (3  $\times$  20 mL). Both extracts were dried with  $\text{MgSO}_4$ , filtered, and concentrated in vacuo. The diastereomeric excesses were measured by NMR spectroscopy as described above, and the diastereomeric ratio, *D*, was calculated according to Sih.<sup>21</sup> By this method, we obtained the *cis*-(2*S*,4*S*)-dioxolane methyl ester (2-(*S*)-benzyloxymethyl)-4-(*S*)-carboxylic acid 1,3-dioxolane methyl ester) as a clear oil in 55% overall yield and >98% diastereomeric excess.

**Modeling of Transition State Analogues in  $\alpha$ -Chymotrypsin.** All modeling was done with Discover, version 2.9.7 (Biosym/MSI, San Diego, CA), using the AMBER force field. We used a distance-dependent dielectric constant of 4.0 and scaled the 1–4 van der Waals interactions by 50%. The distance-dependent dielectric constant damps long-range electrostatic interactions to compensate for the lack of explicit solvation.<sup>48</sup> Results were displayed using Insight II version 95.0 (Biosym/MSI). The starting structure was the X-ray crystal structure of tosylated bovine  $\alpha$ -chymotrypsin<sup>49</sup> obtained from Brookhaven protein data bank (file 2cha). Using the Biopolymer module of Insight II, hydrogen atoms were added to correspond to pH 7.0. Histidines were uncharged, aspartates and glutamates were negatively charged, and arginines and lysines were positively charged. The catalytic histidine (His) was protonated. The tosyl group, which covalently linked to Ser195 in the X-ray structure, was replaced by a phosphonate analogue shown in Figure 6. Energy minimization proceeded in four stages. First, 200 iterations of steepest descent algorithm, all protein atoms constrained with a force constant of 10 kcal mol<sup>-1</sup>  $\text{\AA}^{-2}$ ; second, 200 iterations of conjugate gradients algorithm with the same constraints; and third, 500 iterations of conjugate gradients algorithm with only the backbone constrained by a 10 kcal mol<sup>-1</sup>  $\text{\AA}^{-2}$  force constant. For the fourth stage, minimization was continued using conjugate gradients algorithm without any constraints until the rms deviation reached less than 0.005  $\text{\AA} \text{mol}^{-1}$ . Crystallographic water molecules were included in all minimizations. Water molecules and the substrate were not constrained through any of the minimization cycles.

**Acknowledgment.** We thank NSERC (Canada) and BioChem Pharma Inc. for financial support and Fluka (Buchs, Switzerland), ThermoGen, Inc. (Chicago, IL), Dr. Maarten Egmond (Unilever Research), and Biocatalysts Ltd. (Pontypridd, UK) for gifts of hydrolases. We thank Josée Dugas, Louise Bernier, and Nola Lee (BioChem Pharma) for HPLC separations. We thank A. Christina Löwendahl for preparation of some of the enzyme solutions.

JO990757C

(47) See Table 1 for details.

(48) Weiner, S. J.; Kollman, P. A.; Case, D. A.; Singh, U. C.; Ghio, C.; Alagona, G.; Profeta, S., Jr.; Weiner, P. *J. Am. Chem. Soc.* **1984**, *106*, 765–784.

(49) Birktoft, J. J.; Blow, D. M., *J. Mol. Biol.* **1972**, *68*, 187–240.